GSA Data Repository

Tibetan Plateau insights into >1100℃ crustal melting in the Quaternary

Xiu-Zheng Zhang[1, 2] Qiang Wang[1, 2*] Derek Wyman[3] Andrew C. Kerr[4] Wei Dan[1, 2] Yue Qi[1, 2]

[1] *State Key Laboratory of Isotope Geochemistry, Guangzhou Institute of Geochemistry, Chinese Academy of Sciences, Guangzhou 510640, China*

[2] *CAS Center for Excellence in Deep Earth Science, Guangzhou, 510640, China*

[3] *School of Geosciences, The University of Sydney, NSW 2006, Australia*

[4] *School of Earth and Environmental Sciences, Cardiff University, Cardiff, CF10 3AT, UK*

Corresponding Author: * Qiang Wang, E-mail: wqiang@gig.ac.cn

Includes the following Materials

- Text S1 Analytical methods.
- Figure S1 Photomicrographs of the UHT dacites and granulite enclaves.
- Figure S2 $^{40}Ar/^{39}Ar$ and Zircon U–Pb data.
- Figure S3 (A) Sr/Y versus Y diagram. (B) Zircon saturation temperature versus 10000×Ga/Al diagram.
- Table S1 Representative analyses of minerals of granulite enclaves, peritectic minerals, and phenocrysts of the Dongyue Lake dacites.
- Table S2 Summary of argon isotopic data and ages for the Dongyue Lake dacites.
- Table S3 SIMS zircon U-Pb isotopic results of the Dongyue Lake dacites.
- Table S4 Pb isotopic results of the Dongyue Lake dacites.
- Table S5 Zircon Hf-O isotopic results of the Dongyue Lake dacites.
- Table S6 Calculated heat-production of Devonian–Quaternary felsic rocks from NQB.

Text S1 Analytical Methods

Sample descriptions: All samples analysed and described in this study are from northern Qiangtang, central Tibetan Plateau (Sample 5123-2: N34º25.532', S89º07.661'; Sample 5126-1: N34º23.985', S89º14.676'; Sample 5133: N34º23.275', S89º16.821'; Sample 5124-2: N34º25.203', S89º11.481'; Sample 5127-3: N34º23.393', S89º15.409').

1. Phase Equilibrium

P–T pseudosection has been calculated for the UHT granulite enclave from sample 5123-2 in the NCKFMASHTO (Na_2O–CaO–K_2O–FeO–MgO–Al_2O_3–SiO_2–H_2O–TiO_2–Fe_2O_3) system using the software THERMOCALC, version 3.40i (Powell and Holland, 1988) (updated February, 2012) with dataset ds62 (Holland & Powell, 2011). Mineral activity–composition relationships are the same as those in White et al., (2014) and Wang et al. (2020).

The bulk-rock composition of the enclave melanocratic domain (Opx_{Al} + Ksp + Sp + Ilm; Fig. 2C) was calculated by volume-weighted integration (Opx_{Al} = 45.6 vol%; Ksp = 43.5 vol%; Sp = 7.9 vol%; Ilm =3.0 vol%) of the constituent mineral compositions and is normalized according to the modal system and used for the modelling. Since the mineral assemblage of the melanocratic domain of granulite enclave is completely anhydrous, the H_2O content was adjusted to ensure that the final-phase assemblage occurs just above the dry solidus (Korhonen et al., 2011, 2012; Wang et al., 2020). The oxides were normalized in the NCKFMASHTO system by assuming that P_2O_5 is present in apatite and the O (Fe_2O_3) value equals to the

summation of the Fe^{3+} content in each constituent mineral calculated by charge balance constraints. The input normalized molar proportion used for phase equilibria modelling is: SiO_2 = 50.25 (mol%), Al_2O_3 = 10.59 (mol%), CaO = 0.53 (mol%), MgO = 14.73 (mol%), FeO_2 = 15.33 (mol%), K_2O = 1.89 (mol%), Na_2O = 1.50 (mol%), TiO_2 = 2.33 (mol%), O = 2.60 (mol%), H_2O = 0.25 (mol%).

2. Mineral Chemistry

Representative minerals in the dacites were selected for geochemical analysis by electron probe micro-analyzer (EPMA) JEOL JXA-8800 at State Key Laboratory of Isotope Geochemistry, Guangzhou Institute of Geochemistry, Chinese Academy of Sciences (SKLaBIG GIGCAS). The operating conditions were 20 kV, 20 nA beam current, and 5 μm probe diameter. Representative mineral analyses are listed in Table S1. The structural formulae have been given for fixed oxygen values and with Fe^{3+} calculated by stoichiometric charge balance.

3. ^{40}Ar-^{39}Ar age analyses

Argon isotope analyses were conducted on a GV-5400 mass spectrometer at SKLaBIG GIGCAS. Whole rock chips of 30–60 meshes (1 mesh = 0.254 millimeter) in size and minerals were ultrasonically cleaned first in distilled water with < 5% HNO_3 and then in deionized water, and dried and handpicked to remove visible contamination. The sample and a monitor standard (ZBH-2506 with an age of 132.500 ± 0.663 Ma) were irradiated in the 49-2 reactor in Beijing for 54 h. Details of the analytical procedure used are given in Qiu and Jiang (2007). The ^{40}Ar-^{39}Ar dating results are calculated and plotted using the ArArCALC software of Koppers (2002).

4. CASIMS (Cameca IMS-1280 SIMS) Zircon U-Pb age analyses

Zircons were separated using conventional heavy liquid and magnetic separation techniques. Cathodoluminescence (CL) images were obtained for zircons prior to analysis, using a JEOL JXA-8100 Superprobe at the SKLaBIG GIGCAS, in order to characterize internal structures and choose potential target sites for U-Pb dating.

CASIMS zircon U-Pb analyses were conducted using the Cameca IMS-1280 SIMS at the Institute of Geology and Geophysics, Chinese Academy of Sciences (IGG CAS). Analytical procedures are the same as those described by Li et al. (2009). The O_2^- primary ion beam with an intensity of ca. 10 nA was accelerated at −13 kV. The ellipsoidal spot is about 20 μm × 30 μm in size. The aperture illumination mode (Kohler illumination) was used with a 200 μm primary beam mass filter (PBMF) aperture to produce even sputtering over the entire analyzed area. In the secondary ion beam optics, a 60 eV energy window was used, together with a mass resolution of ca. 5400. Rectangular lenses were activated in the secondary ion optics to in-crease the transmission at high mass resolution. A single electron multiplier was used on ion-counting mode to measure secondary ion beam intensities by peak jumping sequence: 196 ($^{90}Zr_2{}^{16}O$, matrix reference), 200 ($^{92}Zr_2{}^{16}O$), 200.5 (background), 203.81 ($^{94}Zr_2{}^{16}O$, for mass calibration), 203.97 (Pb), 206 (Pb), 207 (Pb), 208 (Pb), 209 ($^{177}Hf^{16}O_2$), 238 (U), 248 ($^{232}Th^{16}O$), 270 ($^{238}U^{16}O_2$), and 270.1 (reference mass), 1.04, 0.56, 4.16, 0.56, 6.24, 4.16, 6.24, 2.08, 1.04, 2.08, 2.08, 2.08, and 0.24 s, respectively. Each measurement consisted of 7 cycles, and the total analytical time is ca. 12 min.

Calibration of Pb/U ratios is relative to the standard zircon TEMORA 2 (417 Ma) (Black et al., 2004) based on an observed linear relationship between ln($^{206}Pb/^{238}U$)

and ln($^{238}U^{16}O_2/^{238}U$) (Whitehouse et al., 1997). U and Th concentrations of unknowns were determined relative to the standard zircon 91500 with Th and U concentrations of ca. 29 and 81 ppm respectively (Wiedenbeck et al., 1995). Measured compositions were corrected for common Pb using non-radiogenic ^{204}Pb. Common Pb is very low, and is largely derived from laboratory contamination introduced during sample preparation (Ireland & Williams, 2003). An average of present-day crustal composition (Stacey & Kramers, 1975) is used for the common Pb. Uncertainties on individual analyses are reported at 1σ level; mean ages for pooled U-Pb analyses are quoted with 95% confidence interval. Data reduction was carried out using the Isoplot/Ex v. 2.49 program (Ludwig, 2003). In this study, we analyzed eight Qinghu (zircon standard) grains yielding a concordia age of 160.0 ± 2.3 Ma (2σ), which is identical to the recommended value of 159.5 ± 0.2 Ma (Li et al., 2013) within analytical uncertainties.

5. In situ Zircon O-Hf isotope analyses

Measurements of O isotopes were conducted using a newly installed Cameca IMS 1280 large-radius SIMS at IGG CAS. The detailed analytical procedures were similar to those described by Li et al. (2009). The measured oxygen isotopic data were corrected for instrumental mass fractionation (IMF) using the Penglai zircon standard ($\delta^{18}O_{VSMOW}$ = 5.3 ‰) (Li et al., 2009). The internal precision of a single analysis generally was better than 0.2 ‰ (1σ) for the $^{18}O/^{16}O$ ratio. The external precision, measured by the reproducibility of repeated analyses of the Penglai standard, is 0.10 ‰ (2σ, n = 24). Ten measurements of the Qinghu zircon standard during the course of this study yielded a mean of $\delta^{18}O$ = 5.48 ± 0.14 ‰ (2σ), which is consistent within analytical errors with the reported value of 5.4 ± 0.2 ‰ (Li et al., 2013)

(Tables S5).

In situ zircon Hf isotopic analyses were carried out at the SKLaBIG GIGCAS using A Neptune, multi-collector, ICP-MS equipped with a Geolas-193 laser ablation system. During analyses, the spot sizes of 32 and 63 μm and a laser repetition rate of 10 Hz with 100 mJ were used. Details of the technique can be found in Wu et al. (2006). During analyses, the $^{176}Hf/^{177}Hf$ ratio of standard zircon (Penglai zircon megacrysts) was 0.282902 ± 0.000014 (2σ, n = 488), similar to the recommended $^{176}Hf/^{177}Hf$ ratio of ~ 0.282906 (Li et al., 2010).

6. Whole-rock Pb isotope analyses

After crushing, fresher rock fractions were selected and subjected to ultrasonic cleaning in distilled water with < 5% HNO_3 and distilled water, dried and handpicked to remove visible contamination, and then pulverized. For Pb isotopic determination, about 100 mg powder was weighed into a Teflon beaker, spiked and dissolved in concentrated HF at 180 °C for 7h. Lead was separated and purified by conventional cation-exchange technique (AG1×8, 200–400 resin) with diluted HBr as an eluant. Total procedural blanks were less than 50pg Pb. Isotopic ratios were measured using a VG-354 mass-spectrometer at the SKLaBIG GIGCAS following procedures described by Zhu et al. (2001). Repeated analyses of three SRM 981 yielded average values of $^{206}Pb/^{204}Pb$ = 16.930 ± 0.0009 (2σ), $^{207}Pb/^{204}Pb$ = 15.483 ± 0.0009 (2σ) and $^{208}Pb/^{204}Pb$ = 36.673 ± 0.0024(2σ).

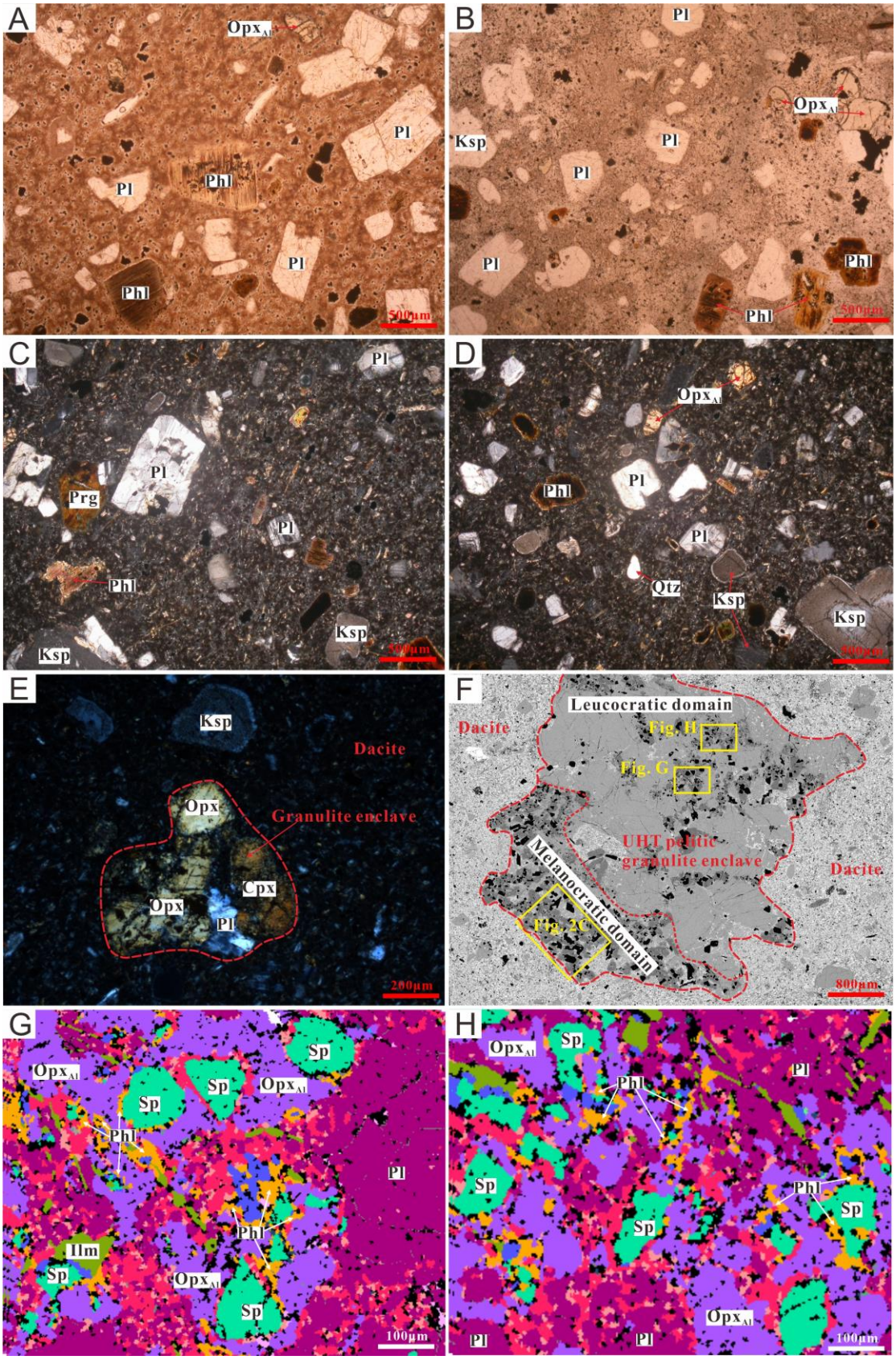

Fig. S1 Photomicrographs of the UHT dacites

(A-D) The Dongyue Lake dacites contain phenocrysts of Pl, Ksp, and Qtz in a cryptocrystalline–glassy groundmass. They record 10–20 vol.% peritectic minerals of

metamorphic origin, including Phl, Opx_{Al}, and minor Prg, which are euhedral–subhedral and almost indistinguishable from phenocrysts in texture. (E) Few samples (e.g., 5123-2) contain minor mafic granulite enclaves with mineral assemblage of Opx + Cpx + Pl. (F) A pelitic granulite enclave from sample 5123-2 is heterogeneous at the millimeter scale and can be divided into melanocratic domains of Opx_{Al} + Sp + Ksp + Ilm and leucocratic domains of Pl + Ksp ± Qtz. (G) and (H) energy-dispersive spectrometry (EDS) phase maps show that Phl occurs locally as a relict mineral which has partially broken down to Opx_{Al} + Sp ± Ilm. Phl = high-F phlogopite, Pl = plagioclase, Opx_{Al} = aluminous orthopyroxene, Opx = orthopyroxene, Cpx = clinopyroxene, Ksp = K-feldspar, Qtz = quartz, Prg = high-F pargasite, Sp = spinel, Ilm = ilmenite. Figs. A, and B are plane polarized light photomicrographs; Figs. C, D, E are crossed-polarized light photomicrographs; Fig. F is back-scattered electron image.

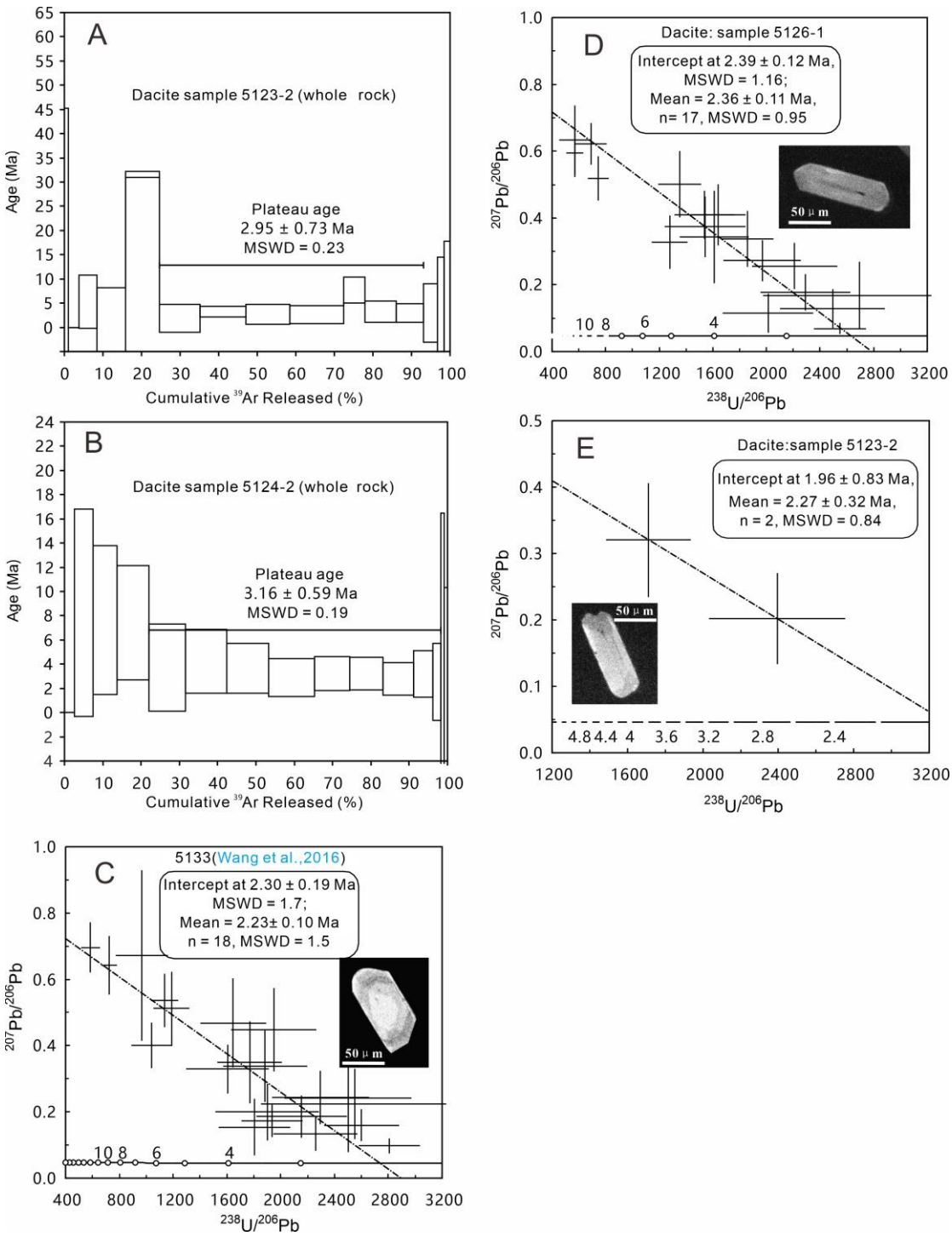

Fig. S2 (A-B) $^{40}Ar/^{39}Ar$ age spectra of whole rocks and phlogopite. (C-E) Zircon U–Pb data of dacites. The slightly older whole-rock $^{40}Ar/^{39}Ar$ age of ca. 3.0 Ma may have been affected by entrainment of peritectic minerals and residual enclaves.

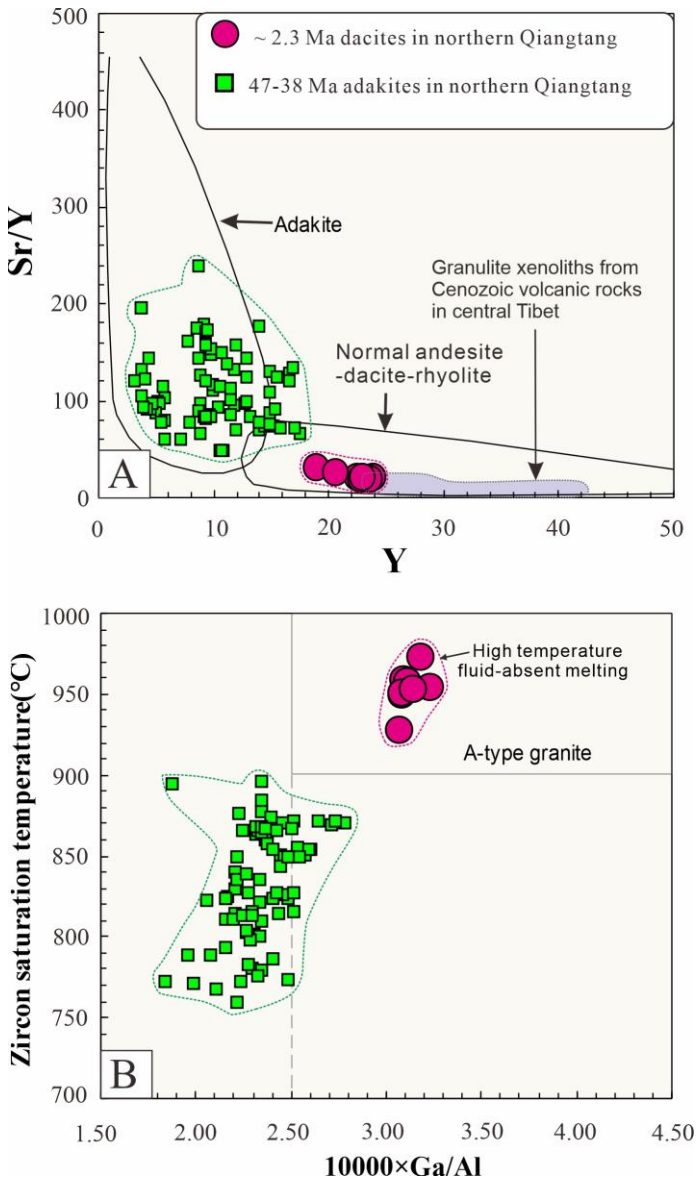

Fig. S3 (A) Sr/Y versus Y diagram. (B) Zircon saturation temperature versus 10000×Ga/Al diagram. Data of granulite xenoliths in the Tibet are after Lai and Qin (2008). 47–38 Ma adakites is from Wang et al. (2008, 2012). Trace-element data of the Dongyue Lake UHT dacites is from our previously study (Wang et al., 2016).

Table S1 Representative analyses of minerals of granulite enclaves, peritectic minerals, and phenocrysts of the Dongyue Lake dacites

	UHT pelitic granulite enclave (Figs. 2 and S1F)															mafic granulite enclave (Figs. S1E)				
Sample	Sample 5123-1															Sample 5123-1				
P-T conditions	T = 1100°C–1150℃, P = 8–9 kbar (P–T pseudosection, Fig.2)															T = 1000°C–1113℃ Cpx-Opx thermometer (Taylor, 1998; Bery and Köhler,1990)				
Mineral	Opx_{Al}	Opx_{Al}	Opx_{Al}	Opx_{Al}	Ksp	Ksp	Ksp	Ksp	Ksp	Ilm	Tim	Sp	Sp	Phl	Phl	Cpx	Cpx	Opx	Opx	Pl
SiO_2	47.49	47.15	46.69	46.86	65.46	65.82	65.63	65.65	65.77	0.03	0.12	0.01	0.03	40.85	39.52	48.79	48.78	52.88	53.97	55.30
TiO_2	0.37	0.30	0.33	0.37	0.15	0.05	0.06	0.10	0.14	48.74	9.05	0.88	0.74	4.42	2.55	1.00	1.02	0.29	0.18	0.05
Al_2O_3	8.32	8.51	9.01	8.88	18.76	19.00	18.53	18.70	18.83	0.35	2.61	52.00	52.79	12.33	12.17	5.99	5.99	3.60	2.18	27.33
FeO	27.42	26.92	26.87	27.15	0.23	0.31	0.44	0.47	0.12	47.02	83.11	38.44	37.00	8.73	8.56	8.06	8.63	14.99	14.89	0.57
MnO	0.47	0.44	0.39	0.41	0.02	0.01	0.00	0.00	0.00	0.47	0.33	0.20	0.23	0.02	0.07	0.15	0.13	0.22	0.25	0.00
MgO	16.75	16.78	16.18	16.09	0.00	0.00	0.00	0.00	0.00	3.29	1.16	9.43	9.62	19.29	20.12	13.83	13.66	26.50	27.24	0.04
CaO	0.14	0.12	0.11	0.12	0.78	0.79	0.70	0.77	0.91	0.00	0.00	0.00	0.00	0.00	0.02	19.30	19.16	1.19	1.10	10.05
Na_2O	0.04	0.08	0.06	0.00	3.97	4.29	4.33	4.42	4.56	0.00	0.00	0.00	0.00	0.81	0.82	0.73	0.77	0.07	0.03	5.13
K_2O	0.01	0.00	0.01	0.00	9.66	9.60	9.80	9.74	9.19	0.01	0.00	0.02	0.02	9.19	9.00	0.00	0.01	0.00	0.00	0.59
F	0.00	0.00	0.00	0.00	0.00	0.00	0.00	0.00	0.00	0.00	0.17	0.00	0.00	5.12	5.33	0.00	0.00	0.00	0.00	0.00
Cl	0.01	0.00	0.02	0.00	0.01	0.00	0.01	0.01	0.00	0.00	0.00	0.00	0.00	0.07	0.12	0.00	0.00	0.01	0.00	0.00
Total	101.00	100.29	99.65	99.89	99.03	99.87	99.49	99.84	99.51	99.91	96.61	100.97	100.43	100.83	98.28	98.02	98.33	99.87	99.91	99.06
O*	6	6	6	6	8	8	8	8	8	3	3	4	4	11	11	6	6	6	6	8
Si	1.80	1.79	1.79	1.79	2.99	2.98	2.99	2.98	2.98	0.00	0.01	0.00	0.00	3.02	2.97	1.85	1.84	1.91	1.94	2.53
Ti	0.01	0.01	0.01	0.01	0.01	0.00	0.00	0.00	0.00	0.93	0.50	0.02	0.02	0.25	0.15	0.03	0.03	0.01	0.00	0.00
Al	0.37	0.38	0.41	0.40	1.01	1.01	0.99	1.00	1.01	0.01	0.17	1.76	1.78	1.08	1.08	0.27	0.27	0.15	0.09	1.47
Fe^{3+}	0.03	0.04	0.01	0.00	0.00	0.00	0.00	0.00	0.00	0.21	2.06	0.27	0.26	0.00	0.07	0.05	0.06	0.02	0.02	0.00
Fe^{2+}	0.83	0.82	0.85	0.87	0.01	0.01	0.02	0.02	0.00	0.78	1.18	0.65	0.62	0.55	0.47	0.20	0.21	0.43	0.43	0.00
Mn	0.01	0.01	0.01	0.01	0.00	0.00	0.00	0.00	0.00	0.01	0.01	0.00	0.01	0.00	0.00	0.00	0.00	0.01	0.01	0.00
Mg	0.94	0.95	0.92	0.92	0.00	0.00	0.00	0.00	0.00	0.12	0.06	0.40	0.41	2.13	2.28	0.78	0.77	1.43	1.46	0.00
Ca	0.01	0.00	0.00	0.00	0.04	0.04	0.03	0.04	0.04	0.00	0.00	0.00	0.00	0.00	0.00	0.78	0.78	0.05	0.04	0.49
Na	0.00	0.01	0.00	0.00	0.35	0.38	0.38	0.39	0.40	0.00	0.00	0.00	0.00	0.12	0.12	0.05	0.06	0.00	0.00	0.45
K	0.00	0.00	0.00	0.00	0.56	0.55	0.57	0.56	0.53	0.00	0.00	0.00	0.00	0.85	0.84	0.00	0.00	0.00	0.00	0.03
F	0.00	0.00	0.00	0.00	0.00	0.00	0.00	0.00	0.00	0.00	0.00	0.00	0.00	1.20	1.27	0.00	0.00	0.00	0.00	0.00
Cl	0.00	0.00	0.00	0.00	0.00	0.00	0.00	0.00	0.00	0.00	0.00	0.00	0.00	0.01	0.02	0.00	0.00	0.00	0.00	0.00
Al^{IV}(Opx)	0.20	0.21	0.21	0.21														0.09	0.06	
X_{An}					0.04	0.04	0.03	0.04	0.05											0.50

	entrained peritectic minerals of metamorphic origin													phenocrysts					
Sample	5126-1	5126-1	5133	5123-2	5123-2	5126-1	5126-1	5133	5133	5123-2	5123-2	5123-2	5123-2	5126-1	5126-1	5133	5133	5123-2	5123-2
Mineral	Phl	Phl	Phl	Phl	Phl	Opx_{Al}	Opx_{Al}	Opx_{Al}	Opx_{Al}	Opx_{Al}	Opx_{Al}	Prg	Prg	Pl	Ksp	Pl	Pl	Ksp	Pl
SiO_2	36.98	38.04	39.03	39.27	39.50	46.98	47.14	47.33	47.61	47.89	47.80	41.87	42.61	59.70	65.09	66.54	60.54	65.61	59.62
TiO_2	2.89	3.03	2.77	3.13	2.63	0.25	0.32	0.33	0.35	0.28	0.25	2.33	1.76	0.06	0.00	0.04	0.04	0.03	0.09
Al_2O_3	12.39	12.69	12.24	12.28	12.26	8.11	8.16	7.88	7.84	7.19	7.95	9.83	9.55	24.65	19.47	18.42	23.71	18.65	24.51
FeO	11.57	10.33	12.02	9.43	9.02	27.38	27.82	28.30	27.34	27.47	26.29	15.19	15.84	0.36	0.27	0.03	0.28	0.06	0.39
MnO	0.08	0.08	0.11	0.00	0.09	0.43	0.36	0.72	0.46	0.51	0.39	0.26	0.29	0.00	0.00	0.02		0.01	
MgO	18.58	18.08	17.64	19.40	18.97	16.31	16.41	15.61	16.16	16.26	17.66	12.19	12.25	0.02			0.01		0.02
CaO	0.28	0.02		0.01	0.02	0.12	0.13	0.11	0.12	0.15	0.16	10.74	10.96	7.32	1.03	0.48	6.43	0.45	7.24
Na_2O	0.70	0.62	0.54	0.81	0.66	0.03	0.01	0.00	0.04	0.02	0.01	2.39	2.13	6.59	4.61	3.96	6.85	3.62	6.11
K2O	8.17	8.80	9.13	8.48	9.04	0.01	0.02	0.00	0.00	0.00	0.01	1.64	1.61	1.36	8.46	10.32	1.48	10.23	1.30
F	5.22	4.95	4.35	5.47	4.79	0.00	0.00	0.00	0.00	0.00	0.00	1.77	1.81	0.00	0.00	0.00	0.00	0.00	0.00
Cl	0.21	0.33	0.32	0.12	0.19	0.00	0.00	0.01	0.00	0.00	0.00	0.14	0.17	0.01	0.00	0.00	0.00	0.00	0.01
Total	97.08	96.97	98.15	98.39	97.15	99.61	100.36	100.28	99.93	99.76	100.51	98.35	99.00	100.08	98.93	99.80	99.34	98.64	99.28
O*	11	11	11	11	11	6	6	6	6	6	6	23	23	23	23	23	23	23	23
Si	2.85	2.94	2.97	2.96	2.99	1.80	1.80	1.81	1.82	1.83	1.81	6.42	6.48	2.68	2.96	3.01	2.72	3.00	2.69
Ti	0.17	0.18	0.16	0.19	0.16	0.01	0.01	0.01	0.01	0.01	0.01	0.27	0.20	0.00	0.00	0.00	0.00	0.00	0.00
Al	1.13	1.15	1.10	1.09	1.09	0.37	0.37	0.36	0.35	0.32	0.35	1.78	1.71	1.30	1.04	0.98	1.26	1.01	1.30
Fe^{3+}	0.15	0.19	0.25	0.07	0.13	0.03	0.03	0.00	0.00	0.00	0.03	0.00	0.00	0.00	0.00	0.00	0.00	0.00	0.00
Fe^{2+}	0.59	0.51	0.53	0.52	0.47	0.85	0.85	0.90	0.87	0.88	0.79	1.95	2.01	0.01	0.01	0.00	0.01	0.00	0.01
Mn	0.01	0.01	0.01	0.00	0.01	0.01	0.01	0.02	0.01	0.02	0.01	0.03	0.04	0.00	0.00	0.00	0.00	0.00	0.00
Mg	2.14	2.18	2.10	2.20	2.19	0.93	0.93	0.89	0.92	0.93	0.99	2.79	2.77	0.00	0.00	0.00	0.00	0.00	0.00
Ca	0.02	0.00	0.00	0.00	0.00	0.00	0.01	0.00	0.01	0.01	0.01	1.77	1.79	0.35	0.05	0.02	0.31	0.02	0.35
Na	0.10	0.09	0.08	0.12	0.10	0.00	0.00	0.00	0.00	0.00	0.00	0.71	0.63	0.57	0.41	0.35	0.60	0.32	0.53
K	0.80	0.78	0.80	0.79	0.83	0.00	0.00	0.00	0.00	0.00	0.00	0.32	0.31	0.08	0.49	0.60	0.08	0.60	0.07
F	1.23	1.27	1.12	1.30	1.18	0.00	0.00	0.00	0.00	0.00	0.00	0.86	0.87	0.00	0.00	0.00	0.00	0.00	0.00
Cl	0.03	0.04	0.04	0.02	0.02	0.00	0.00	0.00	0.00	0.00	0.00	0.04	0.05	0.00	0.00	0.00	0.00	0.00	0.00
Al^{IV}(Opx)						0.20	0.20	0.19	0.18	0.17	0.19								
X_{An}														0.35	0.05	0.02	0.31	0.02	0.36

Note: X_{An} = Ca/ (Ca + Na +K); O*: Assumed number of oxygen atoms per formula unit

Table S2 Summary of argon isotopic data and ages for the Dongyue Lake dacites

Incremental heating		^{36}Ar(a)	^{37}Ar(ca)	^{38}Ar(cl)	^{39}Ar(k)	^{40}Ar(r)	^{40}Ar(r) (%)	^{39}Ar(k) (%)	Age	± 2σ(Ma)
5126-1 high-fluorine phlogopite										
12G2174B	4.20 W	0.000346	0.006351	0.000020	0.000573	0.001028	0.97	0.07	24.24	± 36.99
12G2174C	4.50 W	0.000410	0.000000	0.000093	0.003482	0.001390	1.11	0.41	5.42	± 7.65
12G2174D	4.80 W	0.000336	0.001234	0.000194	0.007007	0.001495	1.45	0.83	2.90	± 2.76
12G2174E	5.10 W	0.000317	0.000000	0.000418	0.014494	0.002450	2.49	1.71	2.30	± 1.20
12G2174F	5.40 W	0.000414	0.000000	0.000920	0.031641	0.004777	3.67	3.73	2.05	± 0.85
12G2174G	5.70 W	0.000137	0.000000	0.000457	0.015763	0.002467	5.62	1.86	2.13	± 1.00
12G2174I	6.20 W	0.000480	0.000000	0.002022	0.070874	0.011282	7.19	8.35	2.16	± 0.53
12G2174J	6.70 W	0.000407	0.000000	0.002497	0.083002	0.013934	10.15	9.78	2.28	± 0.41
12G2174K	7.20 W	0.000449	0.000000	0.002612	0.088160	0.014809	9.82	10.38	2.28	± 0.40
12G2174L	7.70 W	0.000551	0.000000	0.003953	0.131153	0.020998	11.16	15.45	2.18	± 0.29
12G2174M	8.20 W	0.000111	0.000000	0.001072	0.035072	0.005715	14.51	4.13	2.21	± 0.86
12G2174N	8.70 W	0.000220	0.000000	0.002172	0.070292	0.011286	14.46	8.28	2.18	± 0.50
12G2174P	9.20 W	0.000179	0.000000	0.001882	0.061828	0.009982	15.48	7.28	2.19	± 0.60
12G2174Q	9.70 W	0.000198	0.000000	0.002221	0.071665	0.011397	15.88	8.44	2.16	± 0.46
12G2174R	10.00 W	0.000158	0.000000	0.001830	0.057972	0.006131	11.31	6.83	1.44	± 0.61
12G2174S	10.30 W	0.000163	0.000000	0.001798	0.057860	0.006954	12.33	6.81	1.63	± 0.61
12G2174T	10.80 W	0.000083	0.000000	0.000853	0.027918	0.003471	12.09	3.29	1.69	± 1.63
12G2174U	11.30 W	0.000054	0.000000	0.000612	0.020343	0.003671	18.39	2.40	2.45	± 1.59
J= 0.0075378 ±0.0000377, $T_{p(plateau\ age)}$= 2.20 ± 0.15 Ma, $T_{n(normal\ isochron\ age)}$= 2.21 ± 0.30 Ma, $T_{i(inverse\ isochron\ age)}$ = 2.21 ± 0.30 Ma.										
5123-2 whole rock										
12G2172B	4.2 W	0.000625	0.000000	0.000035	0.004218	0.006457	3.38	1.01	19.96	± 25.33
12G2172C	4.5 W	0.000430	0.000000	0.000062	0.011313	0.000000	0.00	2.71	0.00	± 0.00
12G2172D	4.8 W	0.000317	0.000000	0.000101	0.019536	0.007930	7.79	4.68	5.31	± 5.49
12G2172E	5.1 W	0.000319	0.062708	0.000154	0.031259	0.003764	3.84	7.49	1.58	± 6.58
12G2172F	5.4 W	0.000000	0.000000	0.000000	0.036285	0.088195	99.75	8.70	31.58	± 0.68
12G2172G	5.7 W	0.000246	0.000000	0.000187	0.043825	0.006312	7.98	10.50	1.89	± 2.88
12G2172J	6.0 W	0.000204	0.000000	0.000215	0.049858	0.012395	17.01	11.95	3.26	± 1.14
12G2172K	6.3 W	0.000158	0.000000	0.000187	0.047334	0.009537	16.91	11.34	2.64	± 2.07
12G2172L	6.8 W	0.000186	0.000000	0.000256	0.058559	0.011708	17.46	14.03	2.62	± 1.90
12G2172M	7.3 W	0.000257	0.000000	0.000865	0.023218	0.013587	15.17	5.56	7.65	± 2.69
12G2172N	7.8 W	0.000140	0.000000	0.000215	0.033524	0.008351	16.70	8.03	3.26	± 2.20
12G2172O	8.5 W	0.000161	0.000000	0.000238	0.029539	0.006626	12.16	7.08	2.94	± 1.88
12G2172Q	8.8 W	0.000080	0.000000	0.000118	0.014950	0.003364	12.47	3.58	2.95	± 6.04
12G2172R	9.1 W	0.000045	0.000000	0.000067	0.007726	0.001388	9.49	1.85	2.35	± 12.20
12G2172S	9.5 W	0.000040	0.000000	0.000053	0.006138	0.001537	11.43	1.47	3.28	± 14.45
J= 0.0072657 ± 0.0000363, $T_{p(plateau\ age)}$= 2.95 ± 0.73 Ma, $T_{n(normal\ isochron\ age)}$= 2.91 ± 3.87 Ma, $T_{i(inverse\ isochron\ age)}$ = 2.89 ± 3.03 Ma.										
5124-2 whole rock										
12G2173B	4.20 W	0.004440	0.000000	0.000676	0.016240	0.000000	0.00	2.55	0.00	± 0.00
12G2173C	4.50 W	0.004048	0.000000	0.001218	0.030825	0.019028	1.57	4.85	8.24	± 8.56
12G2173D	4.80 W	0.003810	0.011271	0.001516	0.040453	0.023171	2.02	6.36	7.64	± 6.14
12G2173E	5.10 W	0.003802	0.037773	0.001919	0.052922	0.029452	2.55	8.32	7.43	± 4.74

12G2173F	5.40 W	0.003254	0.000000	0.002121	0.060758	0.016918	1.73	9.55	3.72	± 3.60
12G2173G	5.70 W	0.002657	0.000000	0.002325	0.068290	0.021570	2.67	10.74	4.22	± 2.64
12G2173I	6.00 W	0.001935	0.000000	0.002262	0.069383	0.018964	3.21	10.91	3.65	± 2.06
12G2173J	6.30 W	0.001574	0.000000	0.002316	0.076587	0.016450	3.41	12.04	2.87	± 1.57
12G2173K	6.60 W	0.000879	0.000000	0.001643	0.058450	0.014098	5.14	9.19	3.22	± 1.40
12G2173L	6.90 W	0.000655	0.000000	0.001369	0.054476	0.013080	6.32	8.57	3.21	± 1.35
12G2173M	7.20 W	0.000465	0.000000	0.001197	0.051617	0.010819	7.28	8.12	2.80	± 1.34
12G2173N	7.60 W	0.000249	0.000000	0.000609	0.031868	0.007670	9.40	5.01	3.22	± 1.92
12G2173P	8.30 W	0.000097	0.000000	0.000211	0.012796	0.002437	7.80	2.01	2.54	± 3.17
12G2173Q	8.90 W	0.000036	0.017735	0.000105	0.006126	0.002579	19.49	0.96	5.62	± 10.83
12G2173R	9.50 W	0.000036	0.000000	0.000099	0.005229	0.000941	8.03	0.82	2.40	± 7.93

J= 0.0074116 ± 0.0000371, $T_{p(plateau\ age)}$= 3.16 ± 0.59 Ma, $T_{n(normal\ isochron\ age)}$= 2.72 ± 1.15 Ma, $T_{i(inverse\ isochron\ age)}$ = 2.72 ± 1.13 Ma.

Table S3 **SIMS zircon U-Pb isotopic results of the Dongyue Lake dacites**

Sample/ spot #	[U] ppm	[Th] ppm	[Pb] ppm	Th/U meas	$^{238}U/^{206}Pb$	±1σ %	$^{207}Pb/^{206}Pb$	±1σ %	207-corr age (Ma)	±1σ
Sample 5126-1 (This study)										
5126-1@1	155	96	0.19	0.62	1857.94	5.22	0.33796	12.43	2.19	0.22
5126-1@2	98	254	0.19	2.59	1541.94	9.71	0.37343	12.12	2.45	0.34
5126-1@4	89	246	0.20	2.76	1351.99	5.90	0.50080	9.99	2.03	0.33
5126-1@6	105	287	0.10	2.75	2210.43	7.19	0.25628	13.43	2.14	0.20
5126-1@7	144	423	0.74	2.93	691.30	8.58	0.62140	5.06	2.55	0.46
5126-1@8	163	478	0.18	2.93	2291.17	7.30	0.17718	15.30	2.35	0.20
5126-1@9	81	210	0.07	2.58	2494.29	7.85	0.12856	22.54	2.31	0.20
5126-1@11	482	1705	0.42	3.54	2550.27	3.80	0.06884	11.89	2.45	0.10
5126-1@12	101	193	2.10	1.91	185.76	2.40	0.81171	3.63	1.15	1.54
5126-1@13	86	237	0.55	2.74	568.61	5.51	0.59442	5.98	3.49	0.58
5126-1@15	33	58	0.04	1.73	2694.68	13.35	0.16707	30.30	2.03	0.31
5126-1@16	59	157	0.08	2.66	2013.25	8.39	0.11571	25.24	2.92	0.27
5126-1@18	48	115	0.08	2.40	1609.67	7.98	0.34354	20.07	2.50	0.40
5126-1@20	145	440	0.27	3.04	1538.23	7.26	0.40908	8.73	2.27	0.26
5126-1@21	152	463	0.21	3.05	1967.75	7.30	0.27260	11.24	2.34	0.21
5126-1@22	94	238	0.15	2.52	1641.92	6.08	0.40930	11.12	2.13	0.26
5126-1@23	97	200	0.58	2.06	571.00	10.47	0.63409	8.13	2.91	0.82
Sample 5123-2 (This study)										
5123-2@4	99	284	0.11	2.86	2394.80	7.54	0.20166	17.04	2.16	0.20
5123-2@6	82	91	0.11	1.11	1711.57	6.59	0.32010	13.42	2.46	0.26
Samle 5133 (Wang et al., 2016)										
5133@2	156	553	0.16	3.54	2600.83	5.38	0.15986	15.06	2.12	0.14
5133@4	66	167	0.07	2.54	2549.91	13.63	0.22397	23.55	1.96	0.32
5133@5	87	161	0.08	1.85	2500.06	9.43	0.24089	33.49	1.94	0.32
5133@6	402	446	0.22	1.11	2808.39	4.08	0.09801	11.61	2.14	0.09
5133@8	67	148	0.18	2.20	1188.31	5.64	0.51199	10.78	2.23	0.41

5133@9	57	140	0.08	2.46	1883.44	8.30	0.33826	16.03	2.16	0.30
5133@10	91	223	0.10	2.44	2296.43	7.91	0.24351	16.71	2.11	0.22
5133@11	55	127	0.07	2.30	1899.93	10.18	0.19975	21.25	2.73	0.33
5133@12	109	292	0.16	2.69	1605.59	9.59	0.32921	11.31	2.58	0.31
5133@13	50	72	0.18	1.43	966.82	9.94	0.67233	19.13	1.39	1.10
5133@15	96	160	0.08	1.66	2260.02	6.91	0.13361	19.19	2.54	0.20
5133@17	66	161	0.10	2.44	1949.93	8.14	0.44731	14.09	1.63	0.30
5133@18	83	241	0.38	2.90	722.86	4.03	0.64272	6.84	2.20	0.53
5133@19	127	376	0.17	2.95	1934.56	5.85	0.17281	14.28	2.80	0.19
5133@20	74	136	0.08	1.83	2154.14	7.81	0.18614	17.23	2.46	0.23
5133@21	86	228	0.13	2.66	1769.22	6.82	0.34920	17.75	2.25	0.33
5133@24	135	166	0.36	1.23	1138.60	4.47	0.53619	7.50	2.16	0.32
5133@25	46	100	0.08	2.17	1646.68	7.44	0.46851	14.42	1.83	0.36

SIMS Zircon U-Pb zircon standards

Sample/ spot #	[U] ppm	[Th] ppm	[Pb] ppm	Th/U meas	$^{207}Pb/^{235}U$	±1σ %	$^{206}Pb/^{238}U$	±1σ %	$^{207}Pb/^{235}U$	±1σ
Qinghu zircon standard (Mean = 160 ± 2.3 Ma (2σ), n=8 MSWD =0.87)										
Qinghu@8	884	491	27	0.56	0.17027	2.35	0.0249	1.63	159.7	3.5
Qinghu@7	652	313	20	0.48	0.16399	2.77	0.0252	1.52	154.2	4.0
Qinghu@6	776	416	24	0.54	0.17076	2.13	0.0253	1.52	160.1	3.2
Qinghu@5	1076	646	33	0.60	0.16902	2.33	0.0245	1.51	158.6	3.4
Qinghu@4	529	245	16	0.46	0.17224	2.22	0.0251	1.51	161.4	3.3
Qinghu@3	1579	556	46	0.35	0.17092	1.80	0.0254	1.50	160.2	2.7
Qinghu@2	778	316	23	0.41	0.16812	2.04	0.0248	1.52	157.8	3.0
Qinghu@1	1113	692	36	0.62	0.17676	1.97	0.0257	1.58	165.3	3.0
91500 zircon standard										
91500@4	61	22	13	0.36	1.81809	2.80	0.1746	1.50	1052.0	18.5
91500@3	67	24	14	0.36	1.85375	2.14	0.1814	1.51	1064.8	14.2
91500@2	62	22	13	0.36	1.85065	2.12	0.1802	1.50	1063.7	14.1
91500@1	62	22	13	0.36	1.86562	2.13	0.1757	1.51	1069.0	14.2

Table S4 **Pb isotopic results of the Dongyue Lake dacites**

Sample	$^{206}Pb/^{204}Pb$	1sigma SE	$^{207}Pb/^{204}Pb$	1sigma SE	$^{208}Pb/^{204}Pb$	1sigma SE
5123-2	18.820	0.0003	15.745	0.0003	39.336	0.0008
5124-2	18.887	0.0004	15.797	0.0003	39.469	0.0008
5126-1	18.801	0.0002	15.726	0.0002	39.291	0.0006
5127-3	18.859	0.0004	15.775	0.0003	39.424	0.0009
5133	18.818	0.0003	15.739	0.0003	39.329	0.0007
SRM 981 standard						
NBS981-1	16.929	0.0004	15.482	0.0004	36.670	0.0010
NBS981-2	16.930	0.0003	15.483	0.0003	36.673	0.0009
NBS981-3	16.931	0.0004	15.484	0.0003	36.675	0.0011

Table S5 **Zircon Hf-O isotopic results of the Dongyue Lake dacites**

Sample/ spot #	207-corr age (Ma)	±s	$^{176}Yb/^{177}Hf$	$^{176}Lu/^{177}Hf$	$^{176}Hf/^{177}Hf$	±2σ	$\varepsilon_{Hf}(t)$	±2σ	T_{DM2}(Ga)	$\delta^{18}O$	±2σ
Sample 5126-1											
5126-1@1	2.19	0.22	0.010407	0.000247	0.282566	0.000014	-7.24	0.51	1.55	7.62	0.38
5126-1@2	2.45	0.34								7.57	0.35
5126-1@4	2.03	0.33	0.014533	0.00034	0.282504	0.000018	-9.43	0.65	1.69	7.40	0.31
5126-1@6	2.14	0.20	0.017369	0.000447	0.282568	0.000015	-7.17	0.54	1.55	7.11	0.31
5126-1@7	2.55	0.46	0.012155	0.000278	0.282591	0.000014	-6.34	0.51	1.49	7.79	0.36
5126-1@8	2.35	0.20	0.014999	0.000335	0.282685	0.00006	-3.02	2.11	1.28	7.64	0.28
5126-1@9	2.31	0.20	0.022602	0.000544	0.282039	0.000097	-25.89	3.42	2.73	7.45	0.23
5126-1@11	2.45	0.10	0.021392	0.000454	0.282624	0.000015	-5.18	0.52	1.42	7.51	0.18
5126-1@12	1.15	1.54								7.35	0.48
5126-1@13	3.49	0.58								7.25	0.41
5126-1@15	2.03	0.31	0.015823	0.000374	0.282547	0.00002	-7.92	0.71	1.59	7.56	0.23
5126-1@16	2.92	0.27	0.018091	0.000424	0.282617	0.000021	-5.41	0.73	1.43	8.01	0.35
5126-1@18	2.50	0.40	0.012963	0.000312	0.282588	0.00002	-6.45	0.7	1.5	7.05	0.36
5126-1@20	2.27	0.26								7.39	0.46
5126-1@21	2.34	0.21								6.87	0.26
5126-1@22	2.13	0.26	0.020599	0.000495	0.282756	0.000087	-0.53	3.06	1.12	7.48	0.28
5126-1@23	2.91	0.82								7.50	0.28
Sample 5123-2											
5123-2@4	2.16	0.20	0.021649	0.000505	0.282609	0.000018	-5.71	0.63	1.45	7.27	0.29
5123-2@6	2.46	0.26	0.007813	0.000183	0.282608	0.000013	-5.76	0.45	1.46	7.49	0.31
Samle 5133											
5133@2	2.12	0.14								7.28	0.33
5133@4	1.96	0.32	0.016964	0.000397	0.282679	0.000023	-3.24	0.82	1.3	7.55	0.33
5133@5	1.94	0.32								7.42	0.25
5133@6	2.14	0.09	0.009006	0.000233	0.282571	0.000013	-7.06	0.45	1.54	7.90	0.23
5133@8	2.23	0.41								7.35	0.27
5133@9	2.16	0.30	0.011259	0.000275	0.282628	0.000013	-5.03	0.45	1.41	7.86	0.34

5133@10	2.11	0.22	0.015003	0.00037	0.282554	0.000014	-7.64	0.49	1.58	7.79	0.28
5133@11	2.73	0.33	0.015916	0.000401	0.28252	0.000041	-8.85	1.44	1.65	7.53	0.25
5133@12	2.58	0.31								6.81	0.31
5133@13	1.39	1.10	0.017349	0.000508	0.282789	0.000036	0.64	1.27	1.05	7.58	0.38
5133@15	2.54	0.20	0.009568	0.000237	0.282563	0.000015	-7.34	0.53	1.56	7.34	0.33
5133@17	1.63	0.30								7.39	0.33
5133@18	2.20	0.53								6.12	0.42
5133@19	2.80	0.19	0.013927	0.000341	0.282541	0.000048	-8.13	1.7	1.61	7.21	0.21
5133@20	2.46	0.23	0.008846	0.000219	0.282539	0.000014	-8.19	0.5	1.61	7.38	0.27
5133@21	2.25	0.33								7.68	0.47

Zircon oxygen isotopes: Qinghu zircon standard, mean of $\delta^{18}O$ = 5.48 ± 0.14 ‰ (2σ)

	Qinghu@1	Qinghu@2	Qinghu@3	Qinghu@4	Qinghu@5	Qinghu@6	Qinghu@7	Qinghu@8	Qinghu@9	Qinghu@10
$\delta^{18}O$	5.07	5.44	5.2	5.46	5.72	5.41	5.59	5.53	5.47	5.9
±2σ	0.5	0.35	0.39	0.24	0.33	0.29	0.37	0.18	0.23	0.36

Zircon Hf isotopes: Penglai zircon standard, mean of $^{176}Hf/^{177}Hf$ = 0.282902 ± 0.000014 (2σ)

	Penglai@1	Penglai @2	Penglai @3	Penglai @4	Penglai @5	Penglai @6	Penglai @7	Penglai @8	Penglai @9	Penglai @10
$^{176}Hf/^{177}Hf$	0.282917	0.282890	0.282892	0.282871	0.282934	0.282915	0.282925	0.282924	0.282885	0.282870
±2σ	0.000011	0.000012	0.000010	0.000010	0.000010	0.000011	0.000010	0.000011	0.000011	0.000011

$\varepsilon_{Hf}(t) = [^{176}Hf/^{177}Hf_Z/^{176}Hf/^{177}Hf_{CHUR}(t) - 1] \times 10000$.

$^{176}Hf/^{177}Hf_{CHUR}(T) = {}^{176}Hf/^{177}Hf_{CHUR}(0) - {}^{176}Lu/^{177}Hf_{CHUR} \times (e^{\lambda T} - 1)$, $\lambda(^{176}Lu) = 1.867\times10^{-11} yr^{-1}$

$T_{DM-1} = (1/\lambda) \times \ln[1 + (^{176}Hf/^{177}Hf_{DM} - {}^{176}Hf/^{177}HfZ) / (^{176}Lu/^{177}HfDM - {}^{176}Lu/^{177}Hf_Z)]$.

$T_{DM-2}=T_{DM-1} - (T_{DM-1} - T) \times [(f_{CC} - f_Z) / (f_{CC} - f_{DM})]$.

$f_{Lu/Hf} = {}^{176}Hf/^{177}Hf_Z/^{176}Lu/^{177}Hf_{CHUR} - 1$,

where f_{CC}, f_Z and f_{DM} are the $f_{Lu/Hf}$ values of the continental crust, zircon sample and the depleted mantle; subscript Z = analyzed zircon sample, CHUR = chondritic uniform reservoir; DM = depleted mantle.

Table S6 Calculated heat-production of Devonian–Quaternary felsic rocks from NQB

No.	Rocks	Age Ma	C_U ppm	C_{K2O} wt.%	C_{Th} ppm	A_{red} μW/m^3	Mean μW/m^3	References
1			2.39	3.76	12.18	1.75		
2			2.91	3.08	12.51	1.85		
3			2.32	3.59	11.78	1.69		
4			2.44	3.01	12.11	1.70		
5			1.99	2.73	11.60	1.53		
6			1.93	2.04	10.70	1.40		
7	granite	~370-350	2.36	2.95	13.10	1.74	1.66 ± 0.12	Dan et al., 2018
8			1.96	2.69	11.60	1.52		
9			2.50	2.90	12.60	1.74		
10			2.27	2.69	13.40	1.72		
11			2.37	2.51	12.30	1.66		
12			2.70	2.91	12.30	1.77		
13			2.35	2.54	11.30	1.58		
14			3.78	1.76	14.60	2.12		
15			3.55	1.78	14.90	2.08		
16			4.08	1.85	16.46	2.33		
17			3.70	3.24	17.50	2.41		
18	rhyolite	~259-256	4.12	2.80	16.87	2.44	2.28 ± 0.15	Wang et al., 2018
19			3.81	3.46	18.79	2.55		
20			2.91	3.49	16.14	2.14		
21			3.04	3.61	16.41	2.20		
22			3.46	3.16	15.77	2.23		
23			3.59	3.73	25.40	2.97		
24			2.24	3.93	13.60	1.82		
25	granite	~220	3.23	3.69	21.40	2.60	2.36 ± 0.53	Peng et al., 2015
26			1.91	4.00	9.69	1.47		
27			2.57	3.75	24.40	2.64		
28			3.16	3.57	22.90	2.67		
29			2.83	3.77	18.28	2.28		
30			4.05	3.65	13.88	2.29		
31			6.57	3.92	15.09	3.04		
32			3.98	3.61	16.08	2.42		
33			3.93	3.25	19.93	2.64		
34			4.08	3.26	19.85	2.67		
35			4.04	3.25	20.05	2.68		
36			4.16	3.28	19.98	2.71		
37			4.06	3.23	19.61	2.65		

38	adakitic rocks	47-38	3.88	3.27	19.17	2.58	2.96 ± 0.59	Wang et al., 2008,2012
39			4.02	3.21	20.15	2.68		
40			4.07	3.26	19.19	2.63		
41			3.35	4.05	14.54	2.18		
42			5.72	3.76	21.17	3.23		
43			3.76	2.46	15.95	2.26		
44			4.24	4.96	13.98	2.44		
45			4.26	4.07	29.10	3.42		
46			4.12	4.04	28.34	3.33		
47			8.72	4.65	30.22	4.69		
48			7.48	4.55	30.43	4.38		
49			5.02	4.63	21.18	3.12		
50			7.27	4.41	25.40	3.97		
51			6.08	3.92	23.57	3.50		
52			5.67	4.14	21.62	3.28		
53			5.65	4.07	21.11	3.23		
54			4.15	3.15	17.98	2.55		
55			4.16	3.95	29.04	3.38		
56			4.27	4.04	30.12	3.50		
57			4.81	3.34	21.15	2.96		
58			4.71	3.12	23.80	3.10		
59			4.72	3.50	24.68	3.19		
60			5.06	3.46	26.04	3.37		
61			3.81	3.35	12.30	2.09		
62			4.09	3.02	16.42	2.42		
63			4.92	3.51	18.64	2.83		
64	UHT dacite	~2.3 Ma	5.41	4.78	51.64	5.33	5.71 ± 0.22	Wang et al., 2016 and this study
65			5.81	5.10	57.62	5.87		
66			5.66	4.89	55.40	5.67		
67			6.14	4.99	56.81	5.89		
68			5.72	5.13	56.05	5.75		
69			5.82	5.16	56.61	5.81		
70			5.52	5.14	51.47	5.38		
71			6.22	5.26	57.53	5.99		

A_{red} ($\mu W/m^3$) = ρ ($0.0952C_U + 0.0348C_K + 0.0256\ C_{Th}$) (Artemieva et al., 2017). ρ is density in g/cm^3, and C_U, C_{K2O} and C_{Th} are concentrations of radioactive isotopes in ppm, % and ppm, respectively. Commonly, an average density of 2.70 g/cm^3 is used to calculate heat production for granitic rocks (Artemieva et al., 2017).

References

Black, L. P., Kamo, S. L., Allen, C. M., Davis, D. W., Aleinikoff, J. N., Valley, J. W., Mundil, R., Campbell, I. H., Korsch, R. J., Williams, I. S. & Foudoulis, C., 2004, Improved $^{206}Pb/^{238}U$ microprobe geochronology by the monitoring of a trace-element-related matrix effect; SHRIMP, ID-TIMS, ELA-ICP-MS and oxygen isotope documentation for a series of zircon standards: Chemical Geology, v. 205, p. 115–140.

Brey, G.P. and Köhler, T., 1990, Geothermometry in four–phase lherzolites. II. New thermobarometers, and practical assessment of existing thermobarometers: Journal of Petrology, v. 31, p. 1353–1378.

Dan, W., Wang, Q., Zhang, X.Z., Zhang, C., Tang, G.J., Wang, J., Ou, Q., Hao, L.L., Qi, Y., 2018, Magmatic record of Late Devonian arc-continent collision in the northern Qiangtang, Tibet: implications for the early evolution of East Paleo-Tethys Ocean: Lithos, v. 308-309, p. 104–117.

Holland, T. J. B. & Powell, R., 2011, An improved and extended internally-consistent thermodynamic dataset for phases of petrological interest, involving a new equation of state for solids: Journal of Metamorphic Geology, v. 29, p. 333–383.

Ireland, T.R. & Williams, I.S., 2003, Considerations in Zircon Geochronology by SIMS: Reviews in Mineralogy and Geochemistry, v. 53, p. 215–241.

Koppers, A. A. P., 2002, ArArCALC - software for $^{40}Ar/^{39}Ar$ age calculations: Computers & Geosciences, v. 28, p. 605–619.

Korhonen, F. J., Powell, R. & Stout, J. H., 2012, Stability of sapphirine þ quartz in the oxidized rocks of the Wilson Lake terrane, Labrador: calculated equilibria in

NCKFMASHTO: Journal of Metamorphic Geology, v. 30, p. 21–36.

Korhonen, F. J., Saw, A. K., Clark, C., Brown, M. & Bhattacharya, S., 2011, New constraints on UHT metamorphism in the Eastern Ghats Province through the application of phase equilibria modelling and in situ geochronology: Gondwana Research, v. 20, p. 764–781.

Lai, S.C., and Qin, J.F., 2008, Petrology and geochemistry of the granulite xenoliths from Cenozoic Qiangtang volcanic field：Implication for the nature of the lower crust in the northern Tibetan plateau an d the genesis of Cenozoic volcanic rocks: Acta Petrologica Sinica, v. 24, p. 325–336.

Li, X., Tang, G., Gong, B., Yang, Y., Hou, K., Hu, Z., Li, Q., Liu, Y., and Li, W., 2013, Qinghu zircon: A working reference for microbeam analysis of U-Pb age and Hf and O isotopes: Chinese Science Bulletin, v. 58, p. 4647–4654.

Li, X.H., Liu, Y., Li, Q.L., Guo, C.H., and Chamberlain, K.R., 2009, Precise determination of Phanerozoic zircon Pb/Pb age by multicollector SIMS without external standardization: Geochemistry, Geophysics, Geosystems, v. 10, p. Q04010.

Li, X.H., Long, W.G., Li, Q.L., Liu, Y., Zheng, Y.F., Yang, Y.H., Chamberlain, K.R., Wan, D.F., Guo, C.H., Wang, X.C. & Tao, H., 2010, Penglai Zircon Megacrysts: A Potential New Working Reference Material for Microbeam Determination of Hf-O Isotopes and U-Pb Age: Geostandards and Geoanalytical Research, v. 34, p. 117–134.

Ludwig, K. R., 2003, User’s Manual for Isoplot/Ex Version 3.00. In: Ludwig, K. R., ed., A Geochronological Toolkit for Microsoft Excel: Berkeley Geochronology Center Special Publication: Berkeley, p. 41–70.

Peng, T.P., Zhao, G.C., Fan, W.M., Peng, B.X., Mao, Y.S., 2015, Late Triassic granitic magmatism in the Eastern Qiangtang, Eastern Tibetan Plateau: Geochronology, petrogenesis and implications for the tectonic evolution of the Paleo-Tethys: Gondwana Res., v. 27, p. 1497–1508.

Powell, R. & Holland, T.J.B., 1998, An internally consistent dataset with uncertainties and correlations: 3. Applications to geobarometry, worked examples and a computer program: Journal of Metamorphic Geology, v. 6, p. 173–204.

Qiu, H. N. & Jiang, Y. D., 2007, Sphalerite $^{40}Ar/^{39}Ar$ progressive crushing and stepwise heating techniques: Earth and Planetary Science Letters, v. 256, p. 224–232.

Stacey, J. S. & Kramers, J. D., 1975, Approximation of terrestrial lead isotope evolution by a two-stage model: Earth and Planetary Science Letters, v. 26, p. 207–221.

Taylor, W.R., 1998, An experimental test of some geothermometer and geobarometer formulations for upper mantle peridotites with application to the thermobarometry of fertile lherzolites and garnet websterite: Neues Jahrbuch für Mineralogie Abhandlungen, v. 172, p. 381–408.

Wang, J., Wang, Q., Zhang, C., Dan, W., Qi, Y., Zhang, X.-Z., Xia, X.P., 2018, Late Permian bimodal volcanic rocks in the northern Qiangtang Terrane, central Tibet: Evidence for interaction between the Emeishan plume and the Paleo-Tethyan subduction system: Journal of Geophysical Research: Solid Earth, v. 123, p. 6540–6561.

Wang, Q., Wyman, D. A., Xu, J., Dong, Y., Vasconcelos, P. M., Pearson, N., Wan, Y., Dong, H., Li, C., Yu, Y., Zhu, T., Feng, X., Zhang, Q., Zi, F. Chu, Z., 2008, Eocene melting of subducting continental crust and early uplifting of central Tibet: Evidence

from central–western Qiangtang high-K calc-alkaline andesites, dacites and rhyolites: Earth and Planetary Science Letters, v. 272, p. 158–171.

Wang Q., Chung S.L., Li X.H., Wyman D., Li Z.X., Sun W.D., Qiu H.N., Liu Y.S., Zhu Y.T., 2012, Crustal melting and flow beneath northern Tibet: Evidence from Mid-Miocene to Quaternary strongly peraluminous rhyolites in southern Kunlun Range: Journal of Petrology, v. 53, no. 12, p. 2523–2566.

Wang Q., Hawkesworth, C.J., Wymane, D., Chung, S. L., Wug, F. Y., Li, X. H., Li, Z. X., Gou, G. N., Zhang, Z. X., Tang, G. J., Dan, W., Ma, L., Dong, Y. H., 2016, Pliocene–Quaternary crustal melting in central and northern Tibet with new insights into crustal flow: Nature Communications, doi: 10.1038/ncomms11888.

Wang, C., Dai, J., Zhao, X., Li, Y., Graham, S.A., He, D., Ran, B., Meng, J., 2014, Outward growth of the Tibetan Plateau during the Cenozoic: a review: Tectonophysics, v. 621, p. 1–43.

White, R.W., Powell, R. & Johnson, T.E., 2014, The effect of Mn on mineral stability in metapelites revisited: new a–x relations for manganese-bearing minerals: Journal of Metamorphic Geology, v. 32, p. 809–828.

Whitehouse, M. J., Claesson, S., Sunde, T. & Vestin, J., 1997, Ion microprobe U-Pb zircon geochronology and correlation of Archaean gneisses from the Lewisian Complex of Gruinard Bay, northwestern Scotland: Geochimica et Cosmochimica Acta, v. 61, p. 4429–4438.

Wiedenbeck, M., Allé, P., Corfu, F., Griffin, W.L., Meier, M., Oberli, F., von Quadt, A., Roddick, J.C., Spiegel, W., 1995, Three natural zircon standards for U–Th–Pb, Lu–Hf, trace element and REE analyses: Geostandards and Geoanalytical Research, v.

19, p. 1–23.

Wu, F.Y., Yang, Y.H., Xie, L.W., Yang, J.H. and Xu, P., 2006, Hf isotopic compositions of the standard zircons and baddeleyites used in U-Pb geochronology: Chemical Geology, v. 234, no. 1–2, p. 105–126.

Zhu, B. Q., Chen, Y. W. & Peng, J. H., 2001, Lead isotope geochemistry of the urban enviroment in the Pearl River Delta: Apply Geochemistry, v. 16, p. 409–417.